# Unconventional Boundary Conditions
## (From Marshmallows to Plungers – Who Would have Guessed?)

**Tina Dardeno**, **Patrick Logan**, and **Peter Avitabile**, University of Massachusetts Lowell, Lowell, Massachusetts

When performing a modal test, a number of mechanisms are available to approximate free-free boundary conditions. Some test setups may be more difficult to implement than others, but ultimately the effects of the boundary conditions on the actual modes of the system are of concern. An expensive setup may not be any better than an equivalent, inexpensive "Rube Goldberg" approach. In lieu of an expensive setup, a low-cost, easily deployed configuration may be improvised from common objects not native to the test lab. In this article, several different boundary conditions are employed, with two being very, very unconventional. The effects of the supports on the flexible modes are explored through testing with multiple support configurations. Natural frequencies and mode shapes of the modes (flexible and rigid-body modes) are presented. Drive-point frequency response functions for the different support configurations are compared. Some other considerations are discussed relative to the general items of concern when performing these types of free-free modal tests.

Often there is a need to test a structure in a free-free configuration. This is usually one of the more simple boundary conditions to achieve in a test lab. Typically a truly built-in condition is very hard to achieve due to the large, massive, seismic-type anchor that is needed. Free-free conditions are also used many times when correlating test results with a finite-element model; again this is a very easy boundary condition to simulate.

Now it is very easy to say "free-free," but many times how this is achieved in a practical lab setting may actually have an effect on the flexible modes of the system as well as the rigid-body modes themselves.[1] There have been many different approaches to achieve this free-free condition, and some have been very expensive. But the bottom line is how do the test boundary conditions affect the measured frequency, damping and mode shapes for the structure under test. That is the most critical question to answer.[2,3]

In some work involving correlation of test data to the finite-element model, analysts will often just use the analytical truly free condition. While this is very easy to do analytically, the practical reality is that the structure under test will actually have some type of spring support system that really needs to be modeled to be compared to the actual test data, which has an actual "real" support system. If this is ignored, there can be improper characterization of the analytical frequencies and mode shapes identified from the model.

To illustrate some of the problems with the boundary conditions, three structures are evaluated. One is a simple frame structure with very closely spaced frequencies for the first bending and first torsion of the frame, which is a very common test scenario seen in many structures. The second structure is a cantilevered plate attached to a larger mass used to mimic some turbine blade qualification tests. The third structure is a shock-response plate fixture. All of these structures use some very nontraditional test support systems as described in each test case.

## Frame Structure with Marshmallow Supports

The dynamic characterization of the small aluminum frame was determined with the frame placed on four large marshmallows and again with the frame placed on 10 small marshmallows. The marshmallows provide a reasonably good free-free condition, but there is some effect on the type and location of the marshmallows used. Data gathering was performed with the frame located on a seismic anchor (Figure 1).

For the test with four large marshmallows, the marshmallows were placed in the center of each side of the frame, as shown in Figure 1. For the test with 10 small marshmallows, four marshmallows were placed beneath the long end of the frame and one marshmallow was placed beneath the short end of the frame as shown in Figure 1.

Two teardrop accelerometers were placed on the frame: one beneath point 1 and another beneath point 7. A modally tuned impact hammer with a white plastic tip was used to excite the frame at 16 locations. All measurements and impacts were performed in the +Z direction (Figure 2).

Nine flexible modes were evaluated over a bandwidth of 2000 Hz using Photon software via LDS Dactron software. Data were then processed using LMS Test Lab 13 software (Figure 3).

Figure 3 shows that the first and second modes were swapped, depending on the boundary conditions. Specifically, the first and second modes for the four large marshmallow test were bending and torsional modes, respectively. Conversely, for the test with 10 small marshmallows, the first mode was a torsional mode and the second was a bending mode.

The natural frequencies and damping of the two tests are compared in Table 1. This table shows that the natural frequencies associated with the flexible modes remained relatively constant with both boundary conditions. The frequency difference between the first and second modes was greater for the test with 10 small marshmallows (1.72 Hz) compared to the test with four large marshmallows (0.275 Hz), indicating greater overlap of modes for the four large marshmallows. Furthermore, the large marshmallows produced frequencies slightly lower than those obtained with the small marshmallows. This frequency shift implies that the small marshmallow configuration produced greater stiffness than the large marshmallows. However, the large marshmallows produced greater damping for all but the second and fifth modes, compared to the small marshmallow configuration.

From Figure 3, the large marshmallows were located at the node points of the first torsion mode. Different marshmallow locations were selected to create a boundary condition with more of an effect for the first torsion mode. The experiment was repeated with the large marshmallows located at the corners of the frame (Figure 4). The same equipment and testing parameters were used.

Figure 4 shows that moving the four large marshmallows to the corners of the frame resulted in the first torsional mode occurring at a lower frequency than the first bending mode, which was seen in the test with 10 small marshmallows. Figure 5 compares the first two modes of all three tests.



Figure 1. Testing configuration for aluminum frame on four large marshmallows and on 10 small marshmallows.
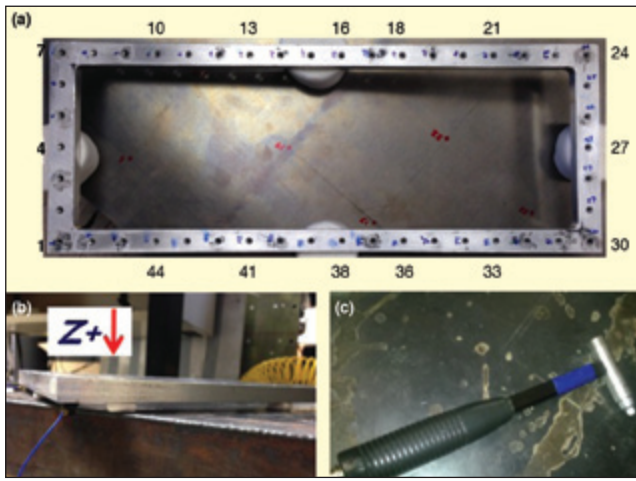
Figure 2. Measurement points and instrumentation for four large marshmallow and 10 small marshmallow tests: (a) Measurement points; (b) Two tear-drop accelerometers, one beneath Point 1 and one beneath Point 7; (c) Modally tuned hammer with white plastic tip.

The natural frequencies and damping of the test with four large marshmallows at the corners are compared to that of the 10 small marshmallows in Table 2. Compared to the 10 small marshmallows, the four large marshmallows at the corners produced lower frequencies. However, the test with four large marshmallows at the corners produced greater damping for all but the second and fifth modes compared to the small marshmallow configuration.

Table 3 compares the natural frequencies and damping of the test with four large marshmallows at the corners to that of the original four large marshmallows. Compared to the original test,
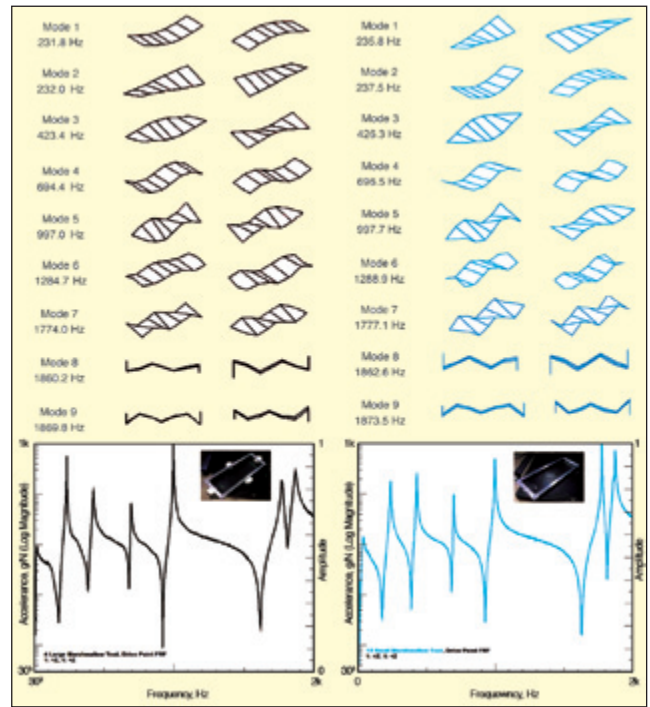


Figure 3. Results of tests with four large marshmallows (left) and 10 small marshmallows (right).

the corner test produced similar frequencies. However, the frequency difference between the first and second modes increased from 0.275 Hz to 3.41 Hz, better aligning with that of the test with

Table 1. Natural frequencies and damping for tests with four large marshmallows and 10 small marshmallows.

| | Frequency, Hz | | | Damping, Percent Critical | | |
|---|---|---|---|---|---|---|
| Mode | Four Large Marshmallows | 10 Small Marshmallows | Percent Difference | Four Large Marshmallows | 10 Small Marshmallows | Percent Difference |
| 1 | 231.766 | 235.784 | 1.72 | 2.31 | 1.14 | 67.83 |
| 2 | 232.041 | 237.502 | 2.33 | 0.16 | 1.12 | 150.00 |
| 3 | 423.397 | 426.309 | 0.69 | 0.96 | 0.43 | 76.26 |
| 4 | 694.349 | 696.520 | 0.31 | 0.38 | 0.29 | 26.87 |
| 5 | 996.980 | 997.680 | 0.07 | 0.07 | 0.27 | 117.65 |
| 6 | 1284.748 | 1288.930 | 0.32 | 0.57 | 0.11 | 135.29 |
| 7 | 1774.023 | 1777.070 | 0.17 | 0.33 | 0.05 | 147.37 |
| 8 | 1860.231 | 1862.640 | 0.13 | 0.37 | 0.18 | 69.09 |
| 9 | 1869.836 | 1873.460 | 0.19 | 0.42 | 0.13 | 105.45 |

Table 2. Natural frequencies and damping for tests with four large marshmallows at corners and 10 small marshmallows.

| | Frequency, Hz | | | Damping | | |
|---|---|---|---|---|---|---|
| Mode | Four Large Marshmallows at Corners | 10 Small Marshmallows | Percent Difference | Four Large Marshmallows at Corners | 10 Small Marshmallows | Percent Difference |
| 1 | 229.910 | 235.784 | 2.52% | 3.11 | 1.14 | 92.71 |
| 2 | 233.318 | 237.502 | 1.78% | 0.76 | 1.12 | 38.30 |
| 3 | 422.352 | 426.309 | 0.93% | 1.55 | 0.43 | 113.13 |
| 4 | 695.133 | 696.520 | 0.20% | 0.15 | 0.29 | 63.64 |
| 5 | 995.690 | 997.680 | 0.20% | 0.35 | 0.27 | 25.81 |
| 6 | 1286.290 | 1288.930 | 0.21% | 0.51 | 0.11 | 129.03 |
| 7 | 1776.203 | 1777.070 | 0.05% | 0.15 | 0.05 | 100.00 |
| 8 | 1855.454 | 1862.640 | 0.39% | 0.60 | 0.18 | 107.69 |
| 9 | 1872.439 | 1873.460 | 0.05% | 0.38 | 0.13 | 98.04 |

Table 3. Natural frequencies and damping for tests with four large marshmallows at corners and four large marshmallows.

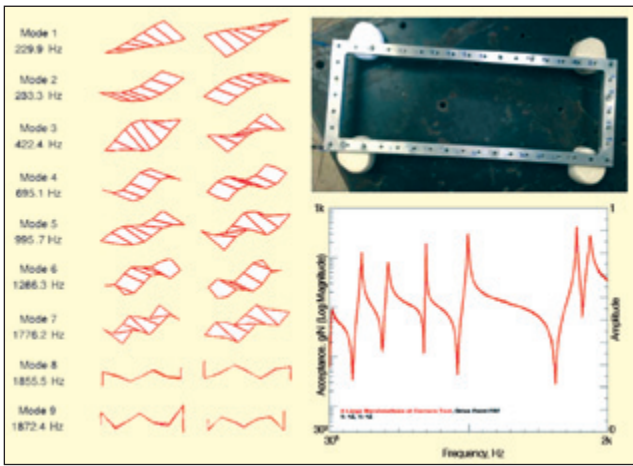| | Frequency, Hz | | | Damping | | |
|---|---|---|---|---|---|---|
| Mode | Four Large Marshmallows at Corners | Four Large Marshmallows | Percent Difference | Four Large Marshmallows at Corners | Four Large Marshmallows | Percent Difference |
| 1 | 229.910 | 231.766 | 0.80% | 3.11 | 2.31 | 29.52 |
| 2 | 233.318 | 232.041 | 0.55% | 0.76 | 0.16 | 130.43 |
| 3 | 422.352 | 423.397 | 0.25% | 1.55 | 0.96 | 47.01 |
| 4 | 695.133 | 694.349 | 0.11% | 0.15 | 0.38 | 86.79 |
| 5 | 995.690 | 996.980 | 0.13% | 0.35 | 0.07 | 133.33 |
| 6 | 1286.290 | 1284.748 | 0.12% | 0.51 | 0.57 | 11.11 |
| 7 | 1776.203 | 1774.023 | 0.12% | 0.15 | 0.33 | 75.00 |
| 8 | 1855.454 | 1860.231 | 0.26% | 0.60 | 0.37 | 47.42 |
| 9 | 1872.439 | 1869.836 | 0.14% | 0.38 | 0.42 | 10.00 |

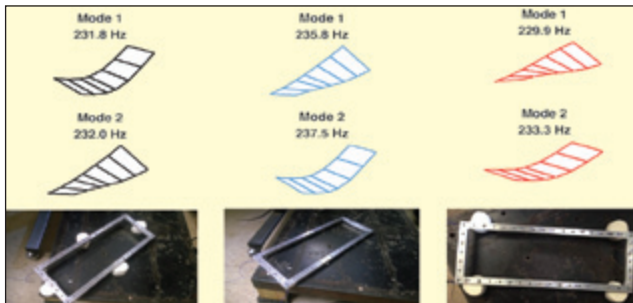*Figure 4. Results of test with four large marshmallows at corners.*



*Figure 5. Results comparison for different marshmallow boundary conditions: Test with four large marshmallows (left); Test with 10 small marshmallows (center); Test with four large marshmallows at corners (right).*

small marshmallows.

The test with large marshmallows at the corners produced greater damping at the first, second, third, fifth, and eighth modes. The increased damping at the first torsional mode is expected, since the marshmallows were moved from the node line to the corners where maximum displacement occurred. Discrepancies in damp-
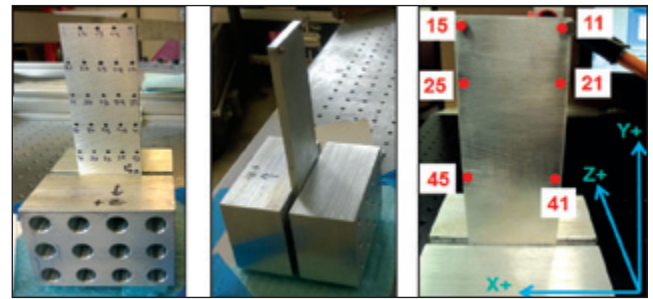


*Figure 6. Calibration structure, from front, side and rear, with impact points and coordinate axes.*

ing at the other modes are likely due to similar movement of the supports either closer to or further from node lines or differences in data processing.

In addition, moving the large marshmallows inward toward the center of the frame produced greater damping. Therefore, differences in how the marshmallows were arranged with respect to the center of the frame may have caused some discrepancy. However, an effort was made to be consistent between the tests. Additional mode comparison for the three tests can be found in Table 4

These three tests show that the boundary condition may have an important effect on the frequencies of the modes as well as the organization and damping of the modes. Therefore, when performing a test on a "free-free" object, one must not only be cautious about the shifting of frequencies but also about the organization of the modes due to the test setup. Overall, the marshmallows provided a very useful free-free boundary condition support.

## Upright Cantilever Calibration Structure on Pads

The upright cantilever calibration structure is a plate bolted into a block with a much larger mass; this is similar to a test configuration for qualification tests of small turbine blades. The structure is generally tested on padded material to minimize the effects of any incompatibilities between the bottom of the structure and the work surface. Experiments with the calibration structure had previously been performed but with different types of padding. In attempting to compare results, the question arose as to the effects of the different types of padding material on the flexible modes.

*Table 4. MAC for all marshmallow tests.*

| | | 4 Large Marshmallows Test | | | | | | | | | 10 Small Marshmallows Test | | | | | | | | | 4 Large Marshmallows at Corners Test | | | | | | | | |
|---|---|---|---|---|---|---|---|---|---|---|---|---|---|---|---|---|---|---|---|---|---|---|---|---|---|---|---|---|
| | | 1 | 2 | 3 | 4 | 5 | 6 | 7 | 8 | 9 | 1 | 2 | 3 | 4 | 5 | 6 | 7 | 8 | 9 | 1 | 2 | 3 | 4 | 5 | 6 | 7 | 8 | 9 |
| 4 Large Marshmallows Test | 1 | 100 | 3.26 | 0.01 | 0.33 | 0.02 | 9.9 | 0 | 0.8 | 3.19 | 7.73 | 92.91 | 0.14 | 0.42 | 0.02 | 8.92 | 0.01 | 0.84 | 4.17 | 0.17 | 97.07 | 0.03 | 0.35 | 0.01 | 8.49 | 0.02 | 0.42 | 3.04 |
| | 2 | 3.26 | 100 | 0.19 | 0.02 | 0.35 | 1.67 | 0.01 | 0.05 | 0.21 | 92.25 | 6.18 | 0.3 | 0.14 | 0.14 | 0.28 | 0.1 | 0.01 | 0.03 | 96.25 | 0.02 | 0.28 | 0.04 | 0.22 | 0.18 | 0.07 | 0.08 | 0.12 |
| | 3 | 0.01 | 0.19 | 100 | 0 | 0.38 | 0.14 | 0.23 | 0.06 | 0 | 0.19 | 0.17 | 99.66 | 0 | 0.46 | 0.21 | 0.06 | 0.02 | 0 | 0.18 | 0.03 | 99.74 | 0 | 0.38 | 0.15 | 0.09 | 0.01 | 0 |
| | 4 | 0.33 | 0.02 | 0 | 100 | 0.13 | 0.32 | 0.07 | 5.55 | 0.39 | 0.03 | 0.35 | 0 | 99.8 | 0.15 | 0.15 | 0.01 | 6.59 | 0.16 | 0.04 | 0.37 | 0 | 99.83 | 0.09 | 0.36 | 0.04 | 6.37 | 0.27 |
| | 5 | 0.02 | 0.35 | 0.38 | 0.13 | 100 | 0.49 | 0.25 | 0.04 | 0.01 | 0.48 | 0.03 | 0.24 | 0.24 | 99 | 0.5 | 0.13 | 0.01 | 0.04 | 0.48 | 0.03 | 0.32 | 0.11 | 98.9 | 0.03 | 0.37 | 0.18 | 0.02 |
| | 6 | 9.9 | 1.67 | 0.14 | 0.32 | 0.49 | 100 | 0.18 | 4.63 | 1.21 | 0.11 | 9.82 | 0.33 | 0.31 | 0.75 | 88.59 | 0.11 | 0.25 | 2.28 | 1.07 | 9.06 | 0.16 | 0.38 | 0.89 | 86.9 | 0.23 | 0.89 | 2.2 |
| | 7 | 0 | 0.01 | 0.23 | 0.07 | 0.25 | 0.18 | 100 | 0.09 | 0.1 | 0.01 | 0.01 | 0.11 | 0.05 | 0.23 | 0.04 | 99.61 | 0.03 | 0.07 | 0.03 | 0 | 0.19 | 0.01 | 0.31 | 0.28 | 99.56 | 0.23 | 0.1 |
| | 8 | 0.8 | 0.05 | 0.06 | 5.55 | 0.04 | 4.63 | 0.09 | 100 | 1.69 | 0.07 | 0.8 | 0.11 | 4.58 | 0.03 | 2.94 | 0.06 | 93.88 | 0.73 | 0.13 | 0.82 | 0.09 | 4.89 | 0.01 | 1.6 | 0.05 | 86.83 | 4.92 |
| | 9 | 3.19 | 0.21 | 0 | 0.39 | 0.01 | 1.21 | 0.1 | 1.69 | 100 | 0.88 | 2.39 | 0 | 0.29 | 0 | 0.58 | 0.01 | 0.87 | 97.36 | 0.23 | 2.98 | 0.01 | 0.4 | 0 | 0.6 | 0.08 | 16.68 | 97.07 |
| 10 Small Marshmallows Test | 1 | 7.73 | 92.25 | 0.19 | 0.03 | 0.48 | 0.11 | 0.01 | 0.07 | 0.88 | 100 | 0.05 | 0.24 | 0.15 | 0.03 | 0.18 | 0.04 | 0.06 | 0.33 | 93.95 | 7.11 | 0.27 | 0.06 | 0.06 | 0.22 | 0.02 | 0.1 | 0.61 |
| | 2 | 92.91 | 6.18 | 0.17 | 0.35 | 0.03 | 9.82 | 0.01 | 0.8 | 2.39 | 0.05 | 100 | 0.54 | 0.51 | 0.01 | 8.01 | 0.07 | 0.69 | 3.61 | 4.92 | 93.66 | 0.27 | 0.37 | 0.01 | 7.63 | 0.06 | 0.28 | 2.38 |
| | 3 | 0.14 | 0.3 | 99.66 | 0 | 0.24 | 0.33 | 0.11 | 0.11 | 0 | 0.24 | 0.54 | 100 | 0 | 0.3 | 0.46 | 0.01 | 0 | 0 | 0.28 | 0.21 | 99.76 | 0 | 0.23 | 0.33 | 0.02 | 0 | 0 |
| | 4 | 0.42 | 0.14 | 0 | 99.8 | 0.24 | 0.31 | 0.05 | 4.58 | 0.29 | 0.15 | 0.51 | 0 | 100 | 0.27 | 0.15 | 0.01 | 5.51 | 0.09 | 0.15 | 0.47 | 0.02 | 99.87 | 0.19 | 0.36 | 0.03 | 5.26 | 0.16 |
| | 5 | 0.02 | 0.14 | 0.46 | 0.15 | 99 | 0.75 | 0.23 | 0.03 | 0 | 0.03 | 0.01 | 0.3 | 0.27 | 100 | 0.41 | 0.11 | 0 | 0.01 | 0.14 | 0.01 | 0.38 | 0.14 | 99.91 | 0.02 | 0.34 | 0.12 | 0 |
| | 6 | 8.92 | 0.28 | 0.21 | 0.15 | 0.5 | 88.59 | 0.04 | 2.94 | 0.58 | 0.18 | 8.01 | 0.46 | 0.15 | 0.41 | 100 | 0.02 | 0.09 | 0.03 | 0.16 | 8.55 | 0.23 | 0.21 | 0.66 | 97.41 | 0.11 | 0.16 | 0.1 |
| | 7 | 0.01 | 0.1 | 0.06 | 0.01 | 0.13 | 0.11 | 99.61 | 0.06 | 0.01 | 0.04 | 0.07 | 0.01 | 0.01 | 0.11 | 0.02 | 100 | 0.01 | 0 | 0.14 | 0.01 | 0.04 | 0.01 | 0.16 | 0.24 | 99.65 | 0.22 | 0.01 |
| | 8 | 0.84 | 0.01 | 0.02 | 6.59 | 0.01 | 0.25 | 0.03 | 93.88 | 0.87 | 0.06 | 0.69 | 0 | 5.51 | 0 | 0.09 | 0.01 | 100 | 0.32 | 0.06 | 0.85 | 0 | 5.79 | 0 | 0.37 | 0 | 87.12 | 0.89 |
| | 9 | 4.17 | 0.03 | 0 | 0.16 | 0.04 | 2.28 | 0.07 | 0.73 | 97.36 | 0.33 | 3.61 | 0 | 0.09 | 0.01 | 0.03 | 0 | 0.32 | 100 | 0.02 | 4.07 | 0 | 0.16 | 0.01 | 0.04 | 0.05 | 10.17 | 97.33 |
| 4 Large Marshmallows at Corners Test | 1 | 0.17 | 96.25 | 0.18 | 0.35 | 0.48 | 1.07 | 0.03 | 0.13 | 0.23 | 93.95 | 4.92 | 0.28 | 0.15 | 0.14 | 0.16 | 0.14 | 0.02 | 0.02 | 100 | 2.93 | 0.26 | 0.04 | 0.22 | 0.26 | 0.09 | 0.06 | 0.11 |
| | 2 | 97.07 | 0.02 | 0.03 | 0.37 | 0.03 | 9.06 | 0 | 0.82 | 2.98 | 7.11 | 93.66 | 0.21 | 0.47 | 0.01 | 8.55 | 0.01 | 0.85 | 4.07 | 2.93 | 100 | 0.06 | 0.37 | 0 | 8.24 | 0.01 | 0.37 | 2.9 |
| | 3 | 0.03 | 0.28 | 99.74 | 0 | 0.32 | 0.16 | 0.19 | 0.09 | 0.01 | 0.27 | 0.27 | 99.76 | 0.02 | 0.38 | 0.23 | 0.04 | 0 | 0 | 0.26 | 0.06 | 100 | 0.01 | 0.3 | 0.16 | 0.07 | 0 | 0 |
| | 4 | 0.35 | 0.04 | 0 | 99.83 | 0.11 | 0.38 | 0.01 | 4.89 | 0.4 | 0.06 | 0.37 | 0 | 99.87 | 0.14 | 0.21 | 0.01 | 5.79 | 0.16 | 0.04 | 0.37 | 0.01 | 100 | 0.08 | 0.41 | 0 | 5.64 | 0.25 |
| | 5 | 0.01 | 0.22 | 0.38 | 0.09 | 98.9 | 0.89 | 0.31 | 0.01 | 0 | 0.06 | 0.01 | 0.23 | 0.19 | 99.91 | 0.66 | 0.16 | 0 | 0.01 | 0.22 | 0 | 0.3 | 0.08 | 100 | 0.01 | 0.42 | 0.1 | 0 |
| | 6 | 8.49 | 0.18 | 0.15 | 0.36 | 0.03 | 86.9 | 0.28 | 1.6 | 0.6 | 0.22 | 7.63 | 0.33 | 0.36 | 0.02 | 97.41 | 0.24 | 0.37 | 0.04 | 0.26 | 8.24 | 0.16 | 0.41 | 0.01 | 100 | 0.44 | 0.21 | 0.08 |
| | 7 | 0.02 | 0.07 | 0.09 | 0.04 | 0.37 | 0.23 | 99.56 | 0.05 | 0.08 | 0.02 | 0.06 | 0.02 | 0.03 | 0.34 | 0.11 | 99.65 | 0 | 0.05 | 0.09 | 0.01 | 0.07 | 0 | 0.42 | 0.44 | 100 | 0.17 | 0.11 |
| | 8 | 0.42 | 0.08 | 0.01 | 6.37 | 0.18 | 0.89 | 0.23 | 86.83 | 4.92 | 0.1 | 0.28 | 0 | 5.26 | 0.12 | 0.16 | 0.22 | 87.12 | 10.17 | 0.06 | 0.37 | 0 | 5.64 | 0.1 | 0.21 | 0.17 | 100 | 17.59 |
| | 9 | 3.04 | 0.12 | 0 | 0.27 | 0.02 | 2.2 | 0.1 | 4.92 | 97.07 | 0.61 | 2.38 | 0 | 0.16 | 0 | 0.1 | 0.01 | 0.89 | 97.33 | 0.11 | 2.9 | 0 | 0.25 | 0 | 0.08 | 0.11 | 17.59 | 100 |
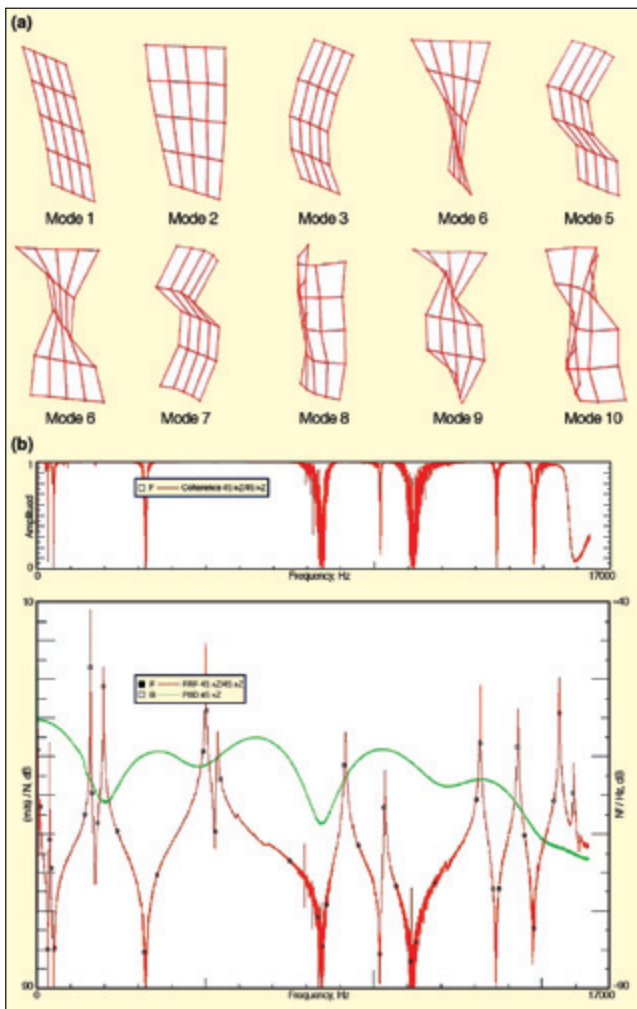
Figure 7. (a) Flexible mode shapes of upright cantilever structure obtained from prior testing; (b) typical coherence, drive-point FRF, and input spectrum obtained during prior testing.
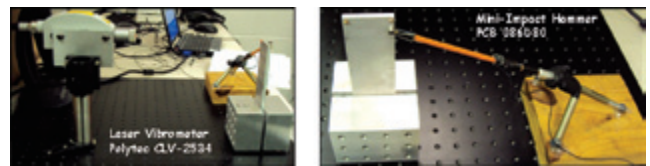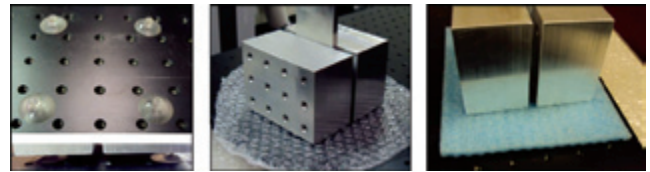


Figure 8. Mini impact hammer and laser setup.



Figure 9. Suction cup, bubble wrap and packing foam used as support padding.



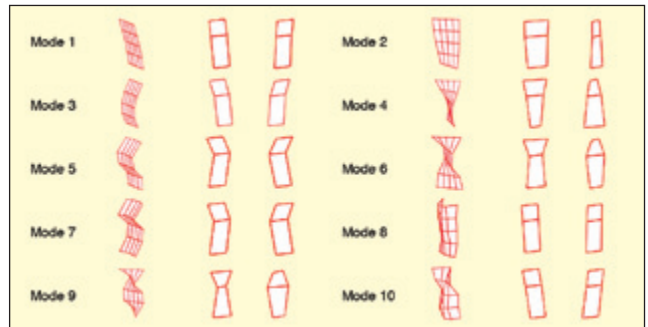Figure 10. Mode shapes of identified flexible modes with prior determined flexible modes as reference.

The structure is shown in Figure 6.

Experimental mode shapes for the structure obtained from prior testing at 25 points are shown in Figure 7a. A drive-point FRF and input and coherence spectra from point 45 are shown in Figure 7b. For this supplemental investigation, six points were selected for study based on the locations of maximum responsiveness of the various flexible modes.

Impact testing was performed with a mini impact hammer at points 11, 15, 21, 25, 41, 45. The impact hammer was mounted to a tripod (with a Dunkin Donuts® straw) to maintain a very consistent impact location on the structure. In addition, impacts at points 11 and 15 were made through ball bearings previously glued to the structure for testing with larger impact hammers; this further controls the accuracy of the impact location. Response was measured at point 11 with a laser. For each point, 10 averages were taken over a 20-kHz bandwidth with a Data Physics Quattro Dynamic Signal Analyzer. Acquisition time was 1.28 seconds for

Table 5. Natural frequencies and modal damping for upright cantilever plate by padding type.

| Mode | Natural Frequency, Hz | | | Damping, Percent | | |
|---|---|---|---|---|---|---|
| | Suction Cups | Bubble Wrap | Foam | Suction Cups | Bubble Wrap | Foam |
| 1 | 370.0 | 371.2 | 369.5 | 0.41 | 0.18 | 0.21 |
| 2 | 1565.6 | 1565.4 | 1565.4 | 0.02 | 0.02 | 0.02 |
| 3 | 1958.2 | 1958.5 | 1957.9 | 0.12 | 0.11 | 0.11 |
| 4 | 4924.3 | 4923.6 | 4923.7 | 0.06 | 0.06 | 0.06 |
| 5 | 5344.8 | 5343.8 | 5344.4 | 0.16 | 0.14 | 0.15 |
| 6 | 9007.4 | 9009.7 | 9008.8 | 0.06 | 0.07 | 0.09 |
| 7 | 10277.0 | 10275.6 | 10276.1 | 0.05 | 0.04 | 0.05 |
| 8 | 12793.3 | 12791.6 | 12792.5 | 0.06 | 0.06 | 0.06 |
| 9 | 13989.2 | 13987.1 | 13988.6 | 0.09 | 0.09 | 0.08 |
| 10 | 15248.2 | 15245.8 | 15245.4 | 0.07 | 0.06 | 0.04 |

Table 6. Natural frequencies and modal damping for tests with three and six plungers.

| Mode | Natural Frequency, Hz | | | | Damping | | |
|---|---|---|---|---|---|---|---|
| | Three Plungers | MAC | Six Plungers | Percent Difference | Three Plungers | Six Plungers | Percent Difference |
| 1 | 4.167 | 77.183 | 4.519 | 8.10 | 6.45 | 6.39 | 0.93 |
| 2 | 4.339 | 93.340 | 4.602 | 5.88 | 6.41 | 6.30 | 1.73 |
| 3 | 5.756 | 91.744 | 6.816 | 16.86 | 6.81 | 7.34 | 7.49 |
| 4 | 9.013 | 94.797 | 9.350 | 3.67 | 5.36 | 8.21 | 42.00 |
| 5 | 10.278 | 90.015 | 12.359 | 18.39 | 5.62 | 10.23 | 58.17 |
| 6 | 13.989 | 91.585 | 15.967 | 13.21 | 6.16 | 9.20 | 39.58 |
| 7 | 219.399 | 94.612 | 217.166 | 1.02 | 0.18 | 1.36 | 153.25 |
| 8 | 315.940 | 88.481 | 316.362 | 0.13 | 0.22 | 0.78 | 112.00 |
| 9 | 439.263 | 80.409 | 439.762 | 0.11 | 0.48 | 1.20 | 85.71 |
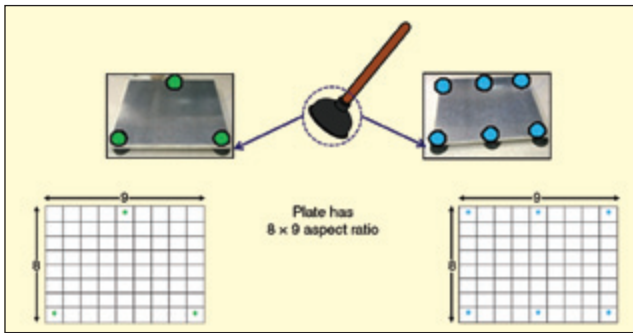
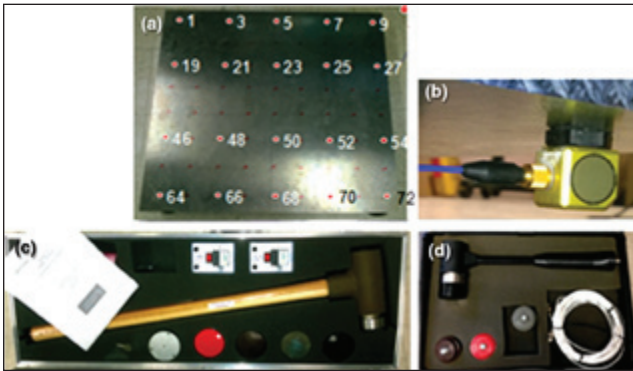Figure 11. Test setup for tests with three plungers (left) and six plungers (right).



Figure 12. (a) Measurement point locations; (b) Tri-axial accelerometer coordinate system; (c) Large sledge used in test with six plungers; (d) Small sledge used in test with three plungers.
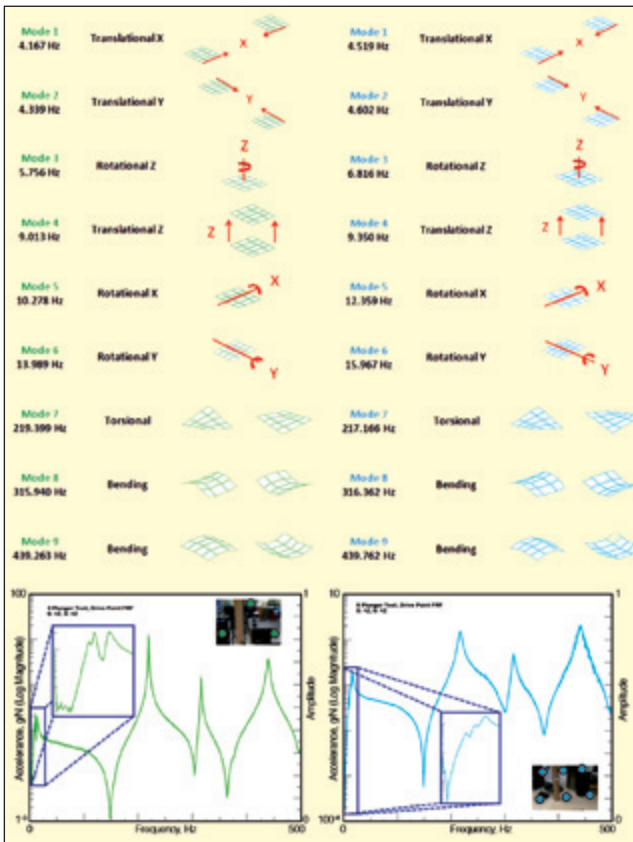


Figure 13. Results of tests with three plungers (left) and six plungers (right).

each measurement. A force-exponential window was employed to reduce the effects of the structure ringing. Data processing was performed using LMS Test Lab 13 software. The impact hammer and laser setup are shown in Figure 8.

The structure was tested on four 3/4-inch-diameter suction cups, bubble wrap and blue packing foam, shown in Figure 9. While bubble wrap and packing foam might routinely be employed, the suction cups were studied as a slightly different mechanism to support the structure. Drive-point FRFs and input spectra were consistent with earlier results.

The frequencies and damping of the identified modes are summarized in Table 5. The identified flexible mode shapes are shown in Figure 10; flexible modes from prior testing are shown for reference.

Table 5 shows little variation in the natural frequencies and modal damping between the suction cups, bubble wrap and foam for the flexible modes. This implies that this boundary condition does not affect the modes of the structure in a significant way; this is largely due to the large attached mass. The large attached mass has the effect of simulating a seismic anchor, so the boundary condition plays a much smaller role in affecting the frequencies and mode shapes. But overall, the suction cups were determined to be the best of the configurations investigated.

## Shock Response Plate Fixture with Plunger Supports

Supporting larger, heavier structures can sometimes be more difficult. Expensive air ride systems or other complicated support mechanisms have often been deployed. Before mounting a new shock plate on an air piston system, a modal test was necessary for some preliminary shock calculations. A good support mechanism that was economical, easy to set up, and would provide useful results was needed.

After some brainstorming, a very different configuration was used – toilet plungers! The dynamic characterization of the aluminum shock response plate was determined with the plate placed on three plungers and again with the plate placed on six plungers (Figure 11). To prevent interference with the accelerometer, for the six-plunger test, the plungers were placed at the edges of the plate. For the three-plunger test, the plungers were positioned directly beneath measurement points.

For the test with three plungers, two plungers were placed at the corners along one of the long sides of the plate, and one plunger was placed in the center of the opposite side (see Figure 11). For the test with six plungers, three plungers were placed along each of the long sides of the plate, as shown in Figure 11.

Measurement points and a coordinate system were defined for both tests. A triaxial accelerometer was placed on the plate beneath point 9. In the test of three plungers, a small sledgehammer with a black plastic tip was used to impact the plate. With the six plungers, a large sledgehammer with a black plastic tip was used. Measurements were acquired in the X, Y, and Z directions as appropriate. The measurement point locations and testing equipment is shown in Figure 12.

The six rigid-body modes and first three flexible modes were evaluated over a bandwidth of 500 Hz using Photon software via LDS Dactron. Data were then processed using LMS Test Lab 13 software. The natural frequencies and damping of the two tests are compared in Table 6. The mode shapes from the plunger tests are shown in Figure 13.

Table 6 shows that using six plungers rather than three plungers increased the frequencies of the six rigid-body modes and the second two flexible modes; decreased the frequency of the first flexible mode; and either increased or decreased the damping depending on the mode. Differences in damping were most noticeable after the first three rigid-body modes. Overall, the toilet plungers were seen to be a very good support configuration for the heavy shock plate and provided very good vertical and lateral support at a cost that is far less than any of the more elaborate pneumatic-isolator systems used.

## References
1. Avitabile, P., "How Free Does a Test Need To Be? Does it Really Matter That Much?" *SEM Experimental Techniques*, August 2012.
2. Avitabile, P., "Can the Test Setup Have an Effect on the Measured Modal Data?" *SEM Experimental Techniques*, December 2001.
3. Avitabile, P., "Will the Support Mechanism Have Any Effect on FRFs? Does Bungie Cord vs. Fishing Line Make Any Difference?" *SEM Experimental Techniques*, December 2010.

SV

Contact the authors at: tina_dardeno@student.uml.edu, patrick_logan@student.uml.edu or peter_avitabile@uml.edu.